

Cooperative metabolic resource allocation in spatially-structured systems

David S. Tourigny*

Columbia University Irving Medical Center
630 West 168th Street, New York, NY 10032 USA

June 3, 2022

Abstract

This paper extends a framework for dynamic metabolic resource allocation based on the maximum entropy principle to spatiotemporal models of metabolism with cooperation. Much like the maximum entropy principle encapsulates ‘bet-hedging’ behaviour displayed by organisms dealing with future uncertainty in a fluctuating environment, its cooperative extension describes how individuals adapt their metabolic resource allocation strategy to further accommodate limited knowledge about the welfare of others within a community. The resulting theory explains why local regulation of metabolic cross-feeding can fulfil a community-wide metabolic objective if individuals take into consideration an ensemble measure of total population performance as the only form of global information. The latter is likely supplied by quorum sensing in microbial systems or signalling molecules such as hormones in multi-cellular eukaryotic organisms.

1 Introduction

Organisms rarely exist in isolation but instead engage in dynamic interaction with their environment and peers as part of a larger population or community. Both environmental and social interactions can have a profound effect on the metabolic behaviour of an individual cell or sub-population, which must often make complex regulatory decisions while faced with uncertainty in many external factors such as nutrient availability. Under these conditions, competition and cooperation commonly emerge due to the pressures of natural selection [1], which further shapes the complexity of biological systems.

Cooperation between microbial cells and populations is generally accepted to be enhanced by spatial structure in the environment, due to limited dispersal and positive assortment keeping cooperators physically clustered together with their partners [2, 3, 4, 5, 6] (however, it is sometimes possible for spatial structure to disfavour cooperation, e.g., [7, 8]). The

*dst2156@cumc.columbia.edu

same is true for metabolic partitioning between intracellular compartments of individual cells [9, 10]. Spatial structure also promotes metabolic cooperation at various levels of organisation in higher-eukaryotic organisms, prominent examples being the well-known Lactic Acid Cycle between liver and muscle [11], the Astrocyte Neuron Lactate Shuttle in brain [12], and the symbiotic production and consumption of lactate by subpopulations of cancer cells within a tumor [13, 14]. The nature of cooperative behaviour displayed in each of these eukaryotic examples is that of ‘metabolic cross-feeding’, which likewise forms an important form of cooperation in microbial communities [15, 16, 17, 18, 19, 20, 21, 22]. Metabolic cross-feeding refers to the process mediated by uptake and exchange of metabolites between individuals or sub-populations, which might invest costly resources to produce metabolites that benefit others in the community rather than using them to fulfil their own metabolic requirements. Cooperative behaviours like metabolic cross-feeding are strategies that can increase the chances of survival and propagation of genes among closely related organisms.

The benefits and exploitation of heterogenous phenotypic traits are also well-appreciated as ‘bet-hedging’ strategies employed by cells and populations dealing with uncertainty in a fluctuating environment [23, 24, 25, 26]. From an economic perspective [27, 28], under these conditions it can be considered sub-optimal to invest metabolic resources exclusively into a single metabolic pathway maximising the metabolic objective. Instead, it can prove advantageous to spread resource among multiple metabolic pathways in a strategic way so as to maximise the expected return, related to using the principle of maximum entropy [29, 30] to formulate resource allocation as an optimality problem. From an information-theoretic standpoint, the distribution of metabolic resources that best represents the current state of knowledge is the one with largest entropy [31], and therefore the maximum entropy distribution is uniquely determined as the one consistent with known constraints but expressing maximum uncertainty with respect to everything else. In biology, the maximum entropy principle has been applied to various resource allocation problems in ecology (see [32] for a review), stem cell multi-potency [33], and a dynamic framework for metabolic resource allocation presented in [34]. The latter was partly motivated by a recent application of the maximum entropy principle to accommodate population heterogeneity in the steady state regime of cellular metabolism [35, 36] and forms a refinement of the work by Young and Ramkrishna [37, 38] (see also earlier work cited therein). This framework unifies previous dynamic models for metabolism, specifically dynamic flux balance analysis (DFBA, [39]) and related unregulated theories [40, 41], and proves successful in describing some observed behaviours of organisms based on first principles alone, including accumulation of metabolite reserves under growth-limiting conditions. Here, the maximum entropy framework is generalised to include models for cooperative metabolic resource allocation in spatially-structured systems, where exploiting heterogeneity and bet-hedging is equally relevant for organisms coping with uncertainty in a temporally-fluctuating environment. It is shown that the cooperative extension of this principle similarly accommodates the limited capacity of an individual cell or sub-population to acquire information about the metabolic activity of other community members outside of their immediate local spatial domain.

The remainder of this paper is organised as follows: Section 2 considers a spatiotemporal model for metabolism that extends the dynamic model in [34] together with a metabolic objective that governs cooperative behaviour. The resulting maximum entropy control law for cooperative resource allocation is introduced in Section 3, which also explores some of

its implications for metabolic cross-feeding. Finally, a concrete application to cooperative behaviour in microbial biofilms and colonies is presented in Section 4. Although the content of this paper is self-contained, many of the principles build upon and complement those considered in [34], therefore readers are encouraged to consult that previous study for reference. Additional mathematical details including the derivation of the cooperative maximum entropy control law can be found in Appendix A.

2 Spatiotemporal metabolism with cooperation

In [34], the following reduced dynamical system was used as a model for the metabolism of a single species in batch culture

$$\frac{d\mathbf{m}}{dt} = x \sum_{k=1}^K r_k(\mathbf{m}) \mathbf{S} \mathbf{Z}^k u_k, \quad \frac{dx}{dt} = x \sum_{k=1}^K r_k(\mathbf{m}) \mathbf{c}^T \mathbf{Z}^k u_k. \quad (1)$$

Here \mathbf{m} ($\text{g} \cdot \text{L}^{-1}$) is an M -dimensional vector of *slow* metabolite concentrations, \mathbf{S} the corresponding ($M \times N$)-dimensional portion of the stoichiometric reaction matrix [42, 43, 44], and the scalar variable x ($\text{gDW} \cdot \text{L}^{-1}$; gDW, grams dry weight) represents the concentration of total catalytic biomass with growth rate (in h^{-1}) determined by the constant coefficient vector $\mathbf{c} = (c_1, c_2, \dots, c_N)^T$ ($\text{gDW} \cdot \text{g}^{-1}$). Obtaining these equations as the reduction of a much larger dynamical system is based on the quasi-steady state assumption (QSSA) [42, 44], which implies metabolites can be separated into two distinct groups based on their dynamic timescales, fast and slow respectively. Under the QSSA, *fast* metabolite concentrations can be considered approximately constant, and the resulting steady state algebraic equations for the N -dimensional flux distribution $\mathbf{v} = (v_1, v_2, \dots, v_N)^T$ ($\text{g} \cdot \text{gDW}^{-1} \cdot \text{h}^{-1}$) are automatically satisfied by expressing \mathbf{v} in terms of the K vectors \mathbf{Z}^k representing elementary flux modes (EFMs) [44]

$$\mathbf{v} = \sum_{k=1}^K r_k(\mathbf{m}) \mathbf{Z}^k u_k.$$

Here $r_k(\mathbf{m})$ denotes the composite flux through the k th EFM and u_k is interpreted as the fraction of total catalytic biomass allocated to the k th EFM due to the finite resource constraint

$$\sum_{k=1}^K u_k = 1, \quad u_k \geq 0 \quad k = 1, 2, \dots, K. \quad (2)$$

A detailed interpretation of $r_k(\mathbf{m})$ and u_k in terms of the molecular biology of enzymes catalysing each metabolic reaction can be found in [34], but is not required for this paper. Here the $r_k(\mathbf{m})$ are simply assumed to be non-negative, smooth functions of the slow metabolite concentrations \mathbf{m} . The u_k are control variables that must be determined in order to satisfy some optimality criteria.

Extending the above model to include spatiotemporal dynamics proceeds by assuming that multiple interacting metabolic systems of the form (1) occupy nodes of a directed graph and that slow metabolites are allowed to be diffusively transported across its edges

[45]. Such models typically arise when discretising reaction-diffusion equations and studying diffusively-coupled chemical reactors or biological cells (e.g., [46, 47, 48]). Abstractly, the graph topology captures spatial organisation in the full spatiotemporal system, and can represent the compartmentalisation of a single cell, tissues or organs in higher-eukaryotes, or spatial structure in the environment or a population of cells. For sake of conciseness, here individual nodes with dynamics (1) will be taken to represent cells or sub-populations in a larger community and the directed graph that encompasses the entire population will be referred to as the *population network*, but application of the model translates to any of the other examples equally well. In the full model consisting of a population network with \mathcal{N} nodes, *local* concentrations of slow metabolites and total catalytic biomass at the i th node will be denoted by \mathbf{m}_i and x_i , respectively, and diffusion of metabolites between nodes is governed by the $(M \times M)$ -dimensional diffusion matrices \mathbf{D}_{ij} (h^{-1}) such that spatiotemporal dynamics of the entire population take the form

$$\frac{d\mathbf{m}_i}{dt} = x_i \sum_{k=1}^{K_i} r_k^i(\mathbf{m}_i) \mathbf{S}_i \mathbf{Z}_i^k u_k^i + \sum_{j=1}^{\mathcal{N}} \mathbf{D}_{ij} \mathbf{m}_j, \quad \frac{dx_i}{dt} = x_i \sum_{k=1}^{K_i} r_k^i(\mathbf{m}) \mathbf{c}_i^T \mathbf{Z}_i^k u_k^i. \quad (3)$$

Super- and subscripts i on \mathbf{S}_i , K_i , \mathbf{c}_i , r_k^i , and \mathbf{Z}_i^k account for possible differences between the genetic or fixed metabolic traits of cells or sub-populations at each node, and have been included here for full generality. They are not necessary when the same species is assumed to inhabit each node of the population network, in which case $\mathbf{S}_i = \mathbf{S}$, $K_i = K$, $\mathbf{c}_i = \mathbf{c}$, $r_k^i = r_k$, and $\mathbf{Z}_i^k = \mathbf{Z}^k$ for all $i = 1, 2, \dots, \mathcal{N}$. Conversely, superscripts i on the u_k^i are always required because they index the different phenotypic or regulatory traits of cells or sub-populations at each node. Components of the vector $\mathbf{u}^i = (u_1^i, u_2^i, \dots, u_K^i)^T$ satisfy the constraint (2) (with K replaced by K_i when considering multiple species), and u_k^i is therefore interpreted as the fraction of local total catalytic biomass at the i th node allocated to the metabolic pathway represented by the k th EFM. The local concentration of total catalytic biomass, x_i , is only able to have an indirect effect on cells or sub-populations at other nodes by contributing to the local production of a slow metabolite, which is then able to diffuse across edges of the population network and participate in metabolic reactions elsewhere.

The metabolic resource allocation strategy \mathbf{u}^i adopted by the cell or sub-population at node i is dependent on maximising some choice of the general metabolic objective function or performance index ϕ_i , which in [34] was taken to be the local concentration of total catalytic biomass, i.e. $\phi_i = x_i$. This metabolic objective assumes that the species at each node acts independently to maximise x_i with complete disregard for cells or sub-populations at other nodes in the population network. In this case \mathbf{u}^i is an example of an *individualist* resource allocation strategy. However, this is not to say there will be no interaction between species using the individualist strategy at different nodes because, as described above, metabolic reactions taking place locally will produce or consume slow metabolites that can diffuse to and participate in reactions at other nodes across the population network, a phenomenon commonly observed in spatially-structured systems that is referred to as metabolic cross-feeding [11, 12, 13, 14, 15, 16, 17, 18, 19, 20, 21, 22]. Metabolic cross-feeding that arises as a consequence of the individualist resource allocation strategy can be interpreted as merely incidental, and is not a cooperative act in the strict sense (i.e., not altruistic) because it comes at no cost to an individual cell or sub-population. However, other instances of metabolic

cross-feeding may be truly cooperative: for example, the cell or sub-population at the i th node might invest resources into producing a metabolite that could otherwise be invested in maximising its own total catalytic biomass, in favour of species at other nodes. Selection for cooperative metabolic cross-feeding in spatially-structured environments is suggested to be facilitated by various factors such as limited or fluctuating nutrient availability and cell population densities [49, 50, 51], in addition to preexistence of incidental metabolic cross-feeding [52]. Cooperative metabolic cross-feeding implies that a *cooperative* resource allocation strategy \mathbf{u}^i is based on some *cooperative metabolic objective* that involves the metabolic performance of cells or sub-populations at other nodes in the population network.

The cooperative metabolic objective considered here is to maximise the generalised mean of total catalytic biomass $\mathbf{x} = (x_1, x_2, \dots, x_{\mathcal{N}})^T$ across the population network, which is given by

$$M_p(\mathbf{x}) = \left(\frac{1}{\mathcal{N}} \sum_{i=1}^{\mathcal{N}} x_i^p \right)^{1/p}. \quad (4)$$

The generalised mean can also come with a set of weightings $\{w_i\}_{i=1,2,\dots,\mathcal{N}}$, one multiplying each x_i and summing to unity, reflecting the fact that different nodes in the population network might not be treated equally. $M_p(\mathbf{x})$ in fact defines a one-parameter family of cooperative objective functions that includes various analogs of the social welfare functions [53] studied in Welfare Economics and Social Choice Theory as special limiting cases of the real parameter p . Interpreted in terms of how the resulting metabolic resource allocation strategy should benefit nodes across the population network, the limiting cases of important relevance are:

- In the limit $p \rightarrow 1$, the metabolic objective becomes maximisation of the arithmetic mean of total catalytic biomass across all nodes in the population network, which is equivalent to the *utilitarian* view that resource at the i th node should be allocated so as to maximise x_i , regardless of the concentrations of total catalytic biomass at others. It turns out that the individualist resource allocation strategy satisfies the utilitarian objective and, as already described, any metabolic cross-feeding that arises as a consequence would therefore be purely incidental
- As $p \rightarrow -\infty$, the generalised mean (4) approaches the minimum function

$$\lim_{p \rightarrow -\infty} M_p(\mathbf{x}) = \min\{x_1, x_2, \dots, x_{\mathcal{N}}\}$$

and the metabolic objective becomes equivalent to the *egalitarian* view that resource should be allocated so as to benefit the node with lowest concentration of total catalytic biomass at any given moment in time. Metabolic cross-feeding resulting from a cooperative resource allocation strategy that satisfies the egalitarian objective would tend to direct metabolites away from nodes already with large x_i to those with lower, and might be expected in systems where it is functionally necessary to maintain existence of cells or sub-populations across the entire population network

- As $p \rightarrow +\infty$, the generalised mean (4) approaches the maximum function

$$\lim_{p \rightarrow +\infty} M_p(\mathbf{x}) = \max\{x_1, x_2, \dots, x_{\mathcal{N}}\}$$

and the objective becomes equivalent to the *elitist* view that resource should be allocated so as to benefit the node with the highest concentration of total catalytic biomass at any given moment in time. In contrast to the egalitarian view, a cooperative resource allocation strategy that satisfies the elitist objective would tend to direct all metabolic cross-feeding towards a single dominant node, with others sacrificing their own growth in its favour. This might be expected in systems where the only matter of importance is to ensure the survival and persistence of a cell or sub-population in at least one location of the population network

- In the limit $p \rightarrow 0$, the objective reduces to maximisation of the geometric mean of total catalytic biomass across all nodes in the population network, equivalent to maximising the *Nash social welfare function* [54], which favours both increases in overall total catalytic biomass across the population network and inequality-reducing metabolic cross-feeding. In this sense, the Nash social welfare objective may be regarded as a good compromise between the utilitarian and egalitarian objectives, and perhaps provides the best example of a cooperative metabolic resource allocation strategy that is mutually beneficial to all nodes in the population network

Introducing a cooperative objective into the spatiotemporal model of metabolic resource allocation poses a potential challenge, because the form of ϕ_i implies that a cell or sub-population at the i th node has access to information pertaining to concentrations of total catalytic biomass *globally* across the entire population network. Although the cooperative resource allocation strategy \mathbf{u}^i is enacted locally, a biological mechanism must exist for obtaining such a global measurement and this could make interpretation or justification of the model difficult. In the case of cells or sub-populations of microbial species however, cooperative decisions are often based on quorum sensing that is well-understood as a general mechanism for signalling population density in spatially-structured environments (see [55] and references therein). Indeed, quorum sensing is known to regulate a wide range of metabolic activity including metabolic cross-feeding [56, 57, 58] and is therefore the clear candidate for communicating concentrations of total catalytic biomass between nodes in the population network. Moreover, integration of metabolism and quorum sensing has recently been shown to govern cooperative behaviour in populations of *Pseudomonas aeruginosa* and other organisms [59, 60]. The way that quorum sensing manifests heterogeneously [61] in response to environmental fluctuations and uncertainty [62] also speaks to the cooperative maximum entropy control introduced in the next section. It is not immediately clear whether such a mechanism exists for multi-cellular organisms, but almost certainly higher-eukaryotes can exploit the circulation of hormones and other signalling molecules for communication between spatially-separated systems.

3 Cooperative maximum entropy control

In [34], a metabolic resource allocation strategy based on the maximum entropy principle was motivated from the perspective of bet-hedging in a temporally-fluctuating environment [23, 24, 25, 26] because, up to a constant factor, entropy uniquely satisfies the accepted axioms for an uncertainty measure [31]. The maximum entropy distribution is therefore

uniquely determined as the one consistent with known constraints (e.g., maximising expected return-on-investment given current environmental conditions) that expresses maximum uncertainty with respect to everything else (e.g., future environmental fluctuations) [29, 30]. Metabolic resource allocation based on the maximum entropy principle and its possible implementation via population heterogeneity [33, 35, 36] is paralleled by the statement that optimal phenotype-switching strategies must accommodate entropies of temporally-fluctuating environments [63]. However, in spatially-structured systems further uncertainty arises due to the physical limit on knowledge that cells or sub-populations can access beyond their immediate local (spatial) environment, and this lack of detailed global information makes cooperative behaviour difficult to understand without an extension of the maximum entropy bet-hedging strategy. In this section, a cooperative maximum entropy control law is derived for a metabolic resource allocation strategy \mathbf{u}^i based on the cooperative metabolic objective of maximising the generalised mean (4). This results in a family of control laws that explain the beneficial properties of metabolic cross-feeding, for various special limiting cases of the parameter p .

Assuming the genetic or fixed traits of species are identical at all nodes in the population network, without loss of generality consider the i th whose dynamics are of the form (3) and resource allocation strategy \mathbf{u}^i is determined by the cooperative metabolic objective function $\phi_i = M_p(\mathbf{x})$. By analogy with [34], the effective return-on-investment for the k th EFM at the i th node is

$$\mathcal{R}_{\Delta t}^{k,i} = \mathbf{q}_i^T \mathbf{e}^{\mathbf{A}\Delta t} \mathbf{B}_i^k \quad (5)$$

where $\mathbf{q}_i = \partial\phi_i(\mathbf{X}(t))/\partial\mathbf{X}$ is the gradient of ϕ_i evaluated at $\mathbf{X}(t) = (\mathbf{m}_1, x_1, \dots, \mathbf{m}_N, x_N)^T$, $\mathbf{e}^{\mathbf{A}\Delta t}$ the matrix exponential of Δt times the full Jacobian matrix \mathbf{A} of system (3) evaluated at $\mathbf{X}(t)$ and reference controls \mathbf{u}_0^i ($i = 1, 2, \dots, \mathcal{N}$), and \mathbf{B}_i^k is the derivative of (3) with respect to u_k^i evaluated at $(\mathbf{m}_i, x_i)^T$. The cooperative maximum entropy control for the i th node is given by

$$u_k^i(t) = \frac{1}{Q_i} \exp\left(\mathcal{R}_{\Delta t}^{k,i}/\sigma\right), \quad k = 1, 2, \dots, K \quad (6)$$

where $Q_i = \sum_{k=1}^K \exp(\mathcal{R}_{\Delta t}^{k,i}/\sigma)$ is a normalisation factor (the partition function) and σ a positive parameter governing the spread of resource among EFMs at the i th node. As described previously [34], the control (6) collapses to the DFBA policy [39] in the limit $\sigma \rightarrow 0$, since then all resource is allocated exclusively to the EFM with the greatest effective return-on-investment (5). Conversely, $u_k^i \rightarrow 1/K$ ($\forall k = 1, 2, \dots, K$) as σ grows so that resource is partitioned equally among all EFMs in the limit $\sigma \rightarrow \infty$. This latter scenario is equivalent to the unregulated macroscopic bioreaction models of Provost and Bastin [40, 41]. Thus, σ captures the bet-hedging nature [23, 24] of dynamic metabolic resource allocation, which could be implemented by exploiting heterogeneity at the population level [25, 35, 36], distributed regulation within each cell [26], or a combination of both mechanisms enacted simultaneously. The maximum entropy control further implies that all EFMs (even those with zero or negative effective return-on-investment) will always be allocated a non-zero fraction of metabolic resource, which distinguishes it from previous resource allocation strategies including those of Young and Ramkrishna [37]. Equipped only with knowledge about the current environment, allocating a small fraction of resource to EFMs not contributing directly to growth is not considered wasteful because there is always a small probability that

these pathways will have a benefit in the future. Appearance of the Jacobian matrix \mathbf{A} in the effective return-on-investment (5) is equivalent to the biological statement that regulatory decisions may also take into consideration effects the control action will have on the environment, and therefore individual EFMs not contributing directly to growth can receive greater (or less) investment should they involve consumption or production of metabolites that make the environment more (or less) favourable. Consequently [34], the maximum entropy principle has been used to explain the accumulation of metabolic reserves under nutrient-limiting conditions [64, 65]. The cooperative maximum entropy control (6) likewise describes the phenomenon of metabolic cross-feeding, analogous to allocation of resources to metabolic pathways that do not contribute directly to the instantaneous growth rate of an individual cell or sub-population, as described below. Stated in terms of cooperative behaviour, this means investment in metabolic pathways that benefit other nodes in the population network at an apparent cost to the i th.

Evaluation of (6) depends on a choice of $\Delta t = 0$, resulting in the *greedy* cooperative maximum entropy control, or $\Delta t > 0$, resulting in the *temporal* cooperative maximum entropy control [37, 34]. The distinction is more than one of computational efficiency, because inclusion of \mathbf{A} in the temporal cooperative maximum entropy control implies that the cell or sub-population at the i th node has knowledge not only about future events, which could be anticipated using some form of regulation, but also specific information pertaining to the level of metabolic activity at nodes elsewhere in the population network. Obtaining the latter may be more difficult to justify on biological grounds. However, although the greedy cooperative maximum entropy control also takes into account both local and global information, the only global information required is an overall measure of the total catalytic biomass across the entire population network. Excluding the utilitarian objective with $p = 1$ (that yields an individualist maximum entropy control identical to [34]), this is most intuitively seen by setting $\Delta t = 0$ in (5) and expressing the greedy effective return-on-investment as (see Appendix A for derivation)

$$\mathcal{R}_0^{k,i} = \frac{x_i^p}{x_i^p + y^p} \cdot M_p(\mathbf{x}) \cdot R_0^k(\mathbf{m}_i). \quad (7)$$

Here $R_0^k(\mathbf{m}) = r_k(\mathbf{m})\mathbf{c}^T\mathbf{Z}^k$ is the zeroth-order return-on-investment for the k th EFM described in [34], and notation y has been introduced for the generalised sum

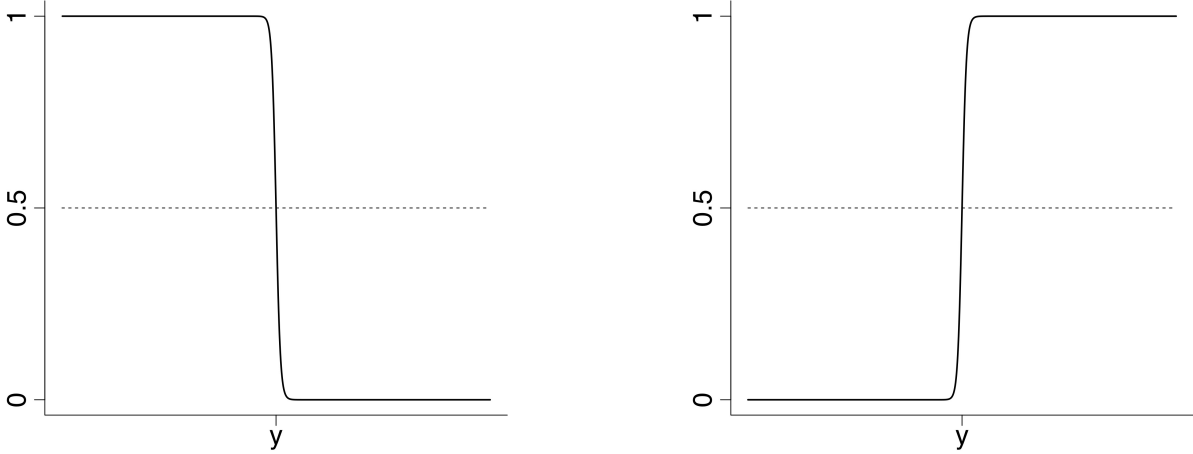
$$y = \left(\sum_{j \neq i}^{\mathcal{N}} x_j^p \right)^{1/p}$$

of total catalytic biomass across the population network not involving the i th node. The terminology *effective* return-on-investment was coined in [34] because, for the greedy individualist maximum entropy control considered there, each u_k came with a common factor of x multiplying $R_0^k(\mathbf{m})/\sigma$ in the exponent. Similarly, for the cooperative control (6) considered here, the greedy effective return-on-investment (7) comes with $R_0^k(\mathbf{m}_i)$ multiplied by two factors: the first, $M_p(\mathbf{x})$, is common to all nodes and EFMs in the population network (i.e., $M_p(\mathbf{x})$ appears in u_k^i for all $i = 1, 2, \dots, \mathcal{N}$, $k = 1, 2, \dots, K$) and therefore plays a role analogous to x in [34], since resource will become further concentrated on the EFMs with

largest $R_0^k(\mathbf{m})$ as the value of the objective function $\phi_i = M_p(\mathbf{x})$ increases. The second, the sigmoid function $x_i^p/(x_i^p + y^p)$, appears as a common factor in the exponent of u_k^i for the i th node (i.e., $x_i^p/(x_i^p + y^p)$ appears in u_k^i for all $k = 1, 2, \dots, K$), but will take on different values at different nodes in accordance with how the local concentration of total catalytic biomass, x_i , compares to the global ensemble, y , as measured across the remainder of the population network. In this sense the greedy cooperative maximum entropy control \mathbf{u}^i requires both local and global information, but does not depend on the cell or sub-population at the i th node having specific knowledge of the metabolic activity or environmental composition at any location other than its own. Instead, only the overall measures of global population network performance provided by y and $M_p(\mathbf{x})$ must be accessible for enacting optimal regulatory decisions locally. As explained in Section 2, an obvious candidate for communicating this information is quorum sensing, which is well-understood as a generic biological mechanism for signalling population density and regulating metabolism in microbial systems [55, 56, 57, 58, 59, 60].

In Figure 1, the sigmoid function in (7) is displayed for low and high values of p where $M_p(\mathbf{x})$ approaches the egalitarian and elitist objective functions, respectively, and illustrates how it approximates a Heaviside step function with change point at y . For the egalitarian regime with $p \ll 0$ the sigmoid $x_i^p/(x_i^p + y^p)$ is close to zero when $x_i > y$, but close to unity when $x_i < y$. This implies that the greedy effective return-on-investment (7) is relatively small when $x_i > y$, which indicates a larger spread of resource across EFMs at the i th node regardless of their zeroth-order return-on-investments $R_0^k(\mathbf{m}_i)$. Consequently, cells or sub-populations whose local concentration of total catalytic biomass is large relative to that of the remaining population will tend to distribute resource more indiscriminately among EFMs, which facilitates metabolic cross-feeding by increasing investment in metabolic pathways that contribute to the production of a metabolite rather than increasing their own local growth rate. Conversely, the greedy effective return-on-investment (7) will be large at nodes with a local concentration of total catalytic biomass that is small relative to that of the remaining population (i.e., when $x_i < y$). Cells or sub-populations at these nodes will instead concentrate their resources on EFMs with large $R_0^k(\mathbf{m})$ in order to maximise their own local concentration of total catalytic biomass directly. The combined effect of this type of cooperative dynamic behaviour will be to increase the total catalytic biomass of the cell or sub-population that has the lowest local concentration across the population network at any given moment in time. When $p \gg 0$, corresponding to the elitist regime, the situation is reversed in that a node with $x_i > y$ will invest greater resource into metabolic pathways maximising x_i , while the spread of resource will be greater and favour production of metabolites for metabolic cross-feeding if $x_i < y$. The combined effect of the cooperative dynamic behaviour that emerges in this case will be to increase the total catalytic biomass of the cell or sub-population with the highest local concentration across the population network at any given moment in time. Between these two extremes is the Nash regime corresponding to $p = 0$, where metabolic cross-feeding is instead controlled uniformly across all nodes in the population network because the common factor of $\frac{1}{2}\sqrt{x_1 x_2 \cdots x_{\mathcal{N}}}$ multiplies $R_0^k(\mathbf{m}_i)/\sigma$ in the exponent of all u_k^i , and therefore plays an equivalent role to x_i in the individualist greedy maximum entropy control. This reflects the compromise between the utilitarian and egalitarian objectives: the cell or sub-population at each node takes into consideration overall population performance when locally regulating the spread of resource

Figure 1: Plots of the sigmoid $x_i^p/(x_i^p + y^p)$ multiplying $M_p(\mathbf{x}) \cdot R_0^k(\mathbf{m}_i)$ as a function of x_i in the greedy effective return-on-investment (7) for low (egalitarian regime) and high (elitist regime) values of p . The value of the generalised sum y is displayed on the x -axis. In the limit $p \rightarrow 0$, the sigmoid converges to the flat line with intercept $1/2$ (represented by dashed line in panels), while for $p = 1$ the denominator of the sigmoid cancels the arithmetic mean $M_1(\mathbf{x})$ and (7) reduces to the greedy effective return-on-investment for the individualistic maximum entropy control [34].



(a) Plot of the sigmoid for $p = -100$.

(b) Plot of the sigmoid for $p = 100$.

across metabolic pathways, and all nodes will tend to favour metabolic cross-feeding (larger spread of resource) when the value of the Nash objective function is low.

The greedy cooperative maximum entropy control law captures several of the relationships between metabolic cross-feeding, nutrient limitation, growth rate, and population density that have been studied previously. Population density has been suggested to determine the conditions that favour metabolic cross-feeding [49, 66], and the same conclusion applies to the cooperative resource allocation strategy considered here if one uses total catalytic biomass to infer population density, which in turn regulates the spread of resource across metabolic pathways as described above. Analogous to the inverse correlation between growth rate and the production of storage metabolites that exists for the individualistic maximum entropy control [34], investment of local resource into pathways producing metabolites for cross-feeding implies a reduction in the local growth rate of the cell or sub-population at the i th node. Reduction of local growth rate is in turn another form of cooperation that provides indirect benefit to neighbouring cells or sub-populations by reducing competition for limited extracellular metabolites [67]; in this sense, the bet-hedging nature of any resource allocation strategy based on the maximum entropy principle can be considered cooperative behaviour in its own right [24]. Recently, Germerodt et al. [51] found that spatially-structured environments with fluctuating nutrient availability tend to favour cooperative metabolic cross-feeding only when metabolites drop below a certain level, which can be explained by appear-

ance of the zeroth-order return-on-investment $R_0^k(\mathbf{m})$ in the greedy return-on-investment (7). As for the individualistic maximum entropy control [34], the greedy cooperative maximum entropy control takes into consideration both the nutrient composition of the environment and concentrations of total catalytic biomass (local versus global), resulting in a metabolic resource allocation strategy determined by the product (7) rather than sum of these quantities. Finally, it is important to highlight that, for the cooperative metabolic objective function (4) considered here, the maximum entropy control law (6) is the only metabolic resource allocation strategy considered to date that will describe such cooperative behaviour in a biologically-realistic setting with $\Delta t = 0$. This follows from the observation that a common factor multiplies $R_0^k(\mathbf{m}_i)$ for all $k = 1, 2, \dots, K$ in the greedy return-on-investment (7), and therefore a DFBA control law obtained from \mathbf{u}^i in the limit $\sigma \rightarrow 0$ would result in all resource being allocated exclusively to the EFM with largest zeroth-order return-on-investment, regardless of the local concentration of total catalytic biomass at the i th node. Similarly, the same multiplicative factor cancels out in the greedy control law derived by Young and Ramkrishna [37], again resulting in a resource allocation strategy that only takes into consideration the $R_0^k(\mathbf{m}_i)$. In their current form, failure of these alternative control laws to account for cooperative metabolic behaviour further supports the original proposal [34] of a model for dynamic metabolic resource allocation based on the maximum entropy principle. This is exemplified by the application described in the next section.

4 Application to microbial biofilms and colonies

This section introduces a model for cooperative metabolic resource allocation in a microbial community consisting of a single species, such as a population of genetically-identical bacteria or yeast growing as a biofilm or colony. These systems often come with a certain degree of spatial organisation because access to nutrients can be limited to particular locations within the total population (e.g., at the extremities of a biofilm or base of a colony) and, consequently, heterogenous phenotypic traits may be adopted by cells or sub-populations occupying different spatial domains. Some of the best-characterised experimental systems are biofilms formed by the pathogenic bacteria *P. aeruginosa* [68, 69], which have motivated several spatiotemporal modelling frameworks that can be used to understand metabolic cross-feeding (e.g., [70, 71, 72]). *P. aeruginosa* is of even greater relevance here, because as a species they are one of the prime examples for which a clear role has been established for quorum sensing in the regulation of cooperative metabolic behaviour [58, 59, 60], possibly including lactate-based metabolic cross-feeding [22]. Other experimental systems to which the model applies equally well, but where a detailed understanding of quorum sensing is comparatively lacking, are colonies of *Escherichia coli* that display a form of acetate-based metabolic cross-feeding [73, 74, 75], and colonies of yeast that exploit similar lactate- [76] or trehalose-based [77] mechanisms.

The model constructed following the framework outlined in previous sections is highly simplified in that the population network consists of just two nodes representing two distinct spatial environments in the colony or biofilm. These are intended to capture either the interior and exterior regions of a three-dimensional biofilm, or the upper and base layers of a raised colony growing on an agar substrate (Figure 2a). The metabolic reaction network

of the microbial species at each node is taken to be a simplified model of central carbon metabolism (Figure 2b and Example 1 in [34], see also [78]), resulting in local concentrations of glucose (G_i), oxygen (O_i), a fermentation product (P_i), and total catalytic biomass (x_i) ($i = 1, 2$ in each case) as kinetic variables. The full dynamical system expressed in terms of the three EFMs (see Example 1 in [34]) corresponding to the following three metabolic pathways: glucose fermentation ($k = 1$); oxidation of the fermentation product ($k = 2$); and oxidation of glucose ($k = 3$), is given by the equations

$$\begin{aligned}
\frac{dG_1}{dt} &= -\frac{1}{2}[r_1(G_1)u_1^1 + r_3(G_1, O_1)u_3^1]x_1 + D_G(G_2 - G_1) \\
\frac{dO_1}{dt} &= kLa(O^* - O_1) - [r_2(O_1, P_1)u_2^1 + r_3(G_1, O_1)u_3^1]x_1 + D_O(O_2 - O_1) \\
\frac{dP_1}{dt} &= [r_1(G_1)u_1^1 - r_2(O_1, P_1)u_2^1]x_1 + D_P(P_2 - P_1) \\
\frac{dx_1}{dt} &= \left[\frac{1}{2}c_1r_1(G_1)u_1^1 + c_3r_2(O_1, P_1)u_2^1 + \frac{1}{2}(c_1 + 2c_3)r_3(G_1, O_1)u_3^1\right]x_1 \\
\\
\frac{dG_2}{dt} &= -\frac{1}{2}[r_1(G_2)u_1^2 + r_3(G_2, O_2)u_3^2]x_2 + D_G(G_1 - G_2) \\
\frac{dO_2}{dt} &= kLa(O^* - O_2) - [r_2(O_2, P_2)u_2^2 + r_3(G_2, O_2)u_3^2]x_2 + D_O(O_1 - O_2) \\
\frac{dP_2}{dt} &= [r_1(G_2)u_1^2 - r_2(O_2, P_2)u_2^2]x_2 + D_P(P_1 - P_2) \\
\frac{dx_2}{dt} &= \left[\frac{1}{2}c_1r_1(G_2)u_1^2 + c_3r_2(O_2, P_2)u_2^2 + \frac{1}{2}(c_1 + 2c_3)r_3(G_2, O_2)u_3^2\right]x_2
\end{aligned}$$

where volumetric mass transfer coefficient kLa and dissolved oxygen solubility limit O^* have been introduced to model oxygen supply, and D_G, D_O, D_P are the diffusion coefficients of extracellular glucose, oxygen, and the fermentation product, respectively. As described in [34], the r_k are approximated by Michaelis-Menten kinetics according to the metabolites whose uptake fluxes are in the support of each EFM, such that

$$\begin{aligned}
r_1(G_i) &= V_1^{max} \frac{G_i}{K_1 + G_i} \\
r_2(O_i, P_i) &= V_2^{max} \frac{P_i}{K_2 + P_i} \frac{O_i}{K_{O,2} + O_i} \\
r_3(G_i, O_i) &= V_3^{max} \frac{G_i}{K_3 + G_i} \frac{O_i}{K_{O,3} + O_i}
\end{aligned}$$

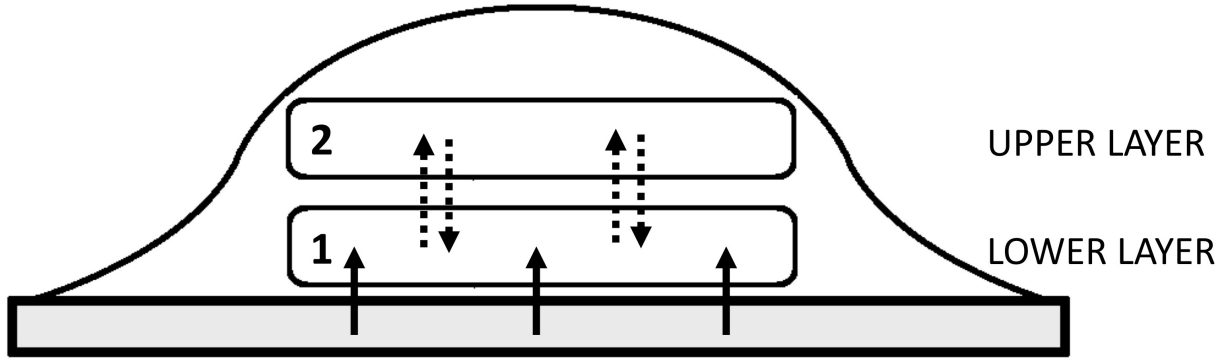
and consequently the zeroth-order return-on-investments are

$$R_0^1(G_i) = \frac{1}{2}c_1r_1(G_i), \quad R_0^2(O_i, P_i) = c_3r_2(O_i, P_i), \quad R_0^3(G_i, O_i) = \frac{1}{2}(c_1 + 2c_3)r_3(G_i, O_i)$$

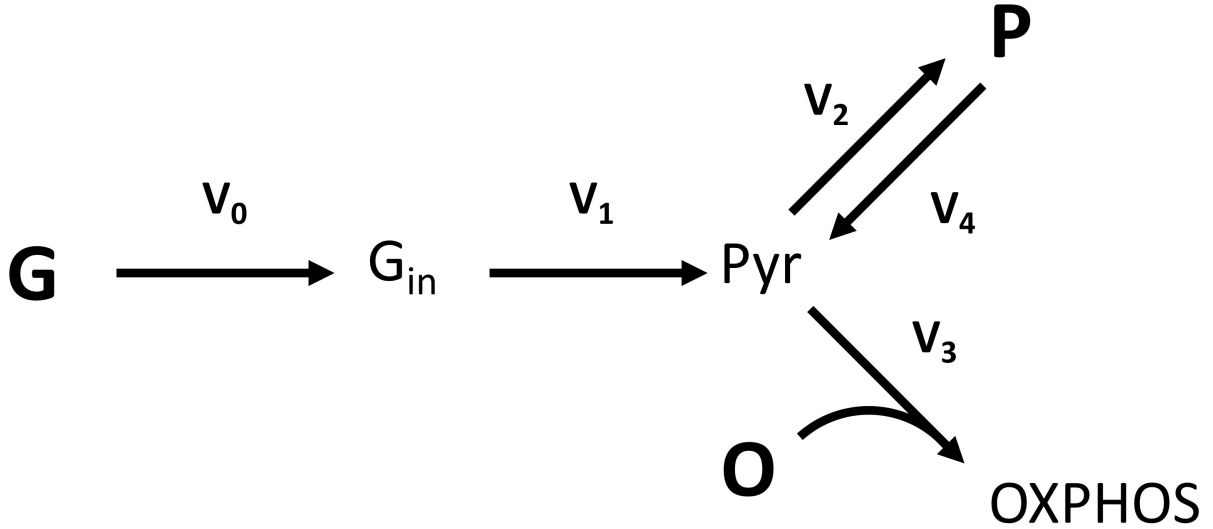
for $i = 1, 2$. The greedy cooperative maximum entropy control law for determining each u_k^i is then

$$u_k^i = \frac{1}{Q_i} \exp\left(\frac{1}{\sigma} \frac{x_i^p}{x_i^p + y^p} \cdot M_p(\mathbf{x}) \cdot R_0^k(\mathbf{m}_i)\right), \quad y = x_{j \neq i}$$

Figure 2: Cartoon illustrations of the population network and metabolic reaction network in the simple model for a microbial biofilm or colony considered in Section 4.



(a) Biological interpretation of the model for a microbial colony growing on an agar substrate containing glucose as a limiting nutrient. Spatial structure of the colony can be approximated as a lower and upper layer, represented by nodes $i = 1$ and $i = 2$ in the population network, respectively. Only cells in the lower layer that is in contact with the agar substrate have access to glucose (represented by solid arrows), while oxygen and the fermentation product (represented by dashed arrows) are free to diffuse between both layers.



(b) Diagrammatic representation of the simplified metabolic reaction network used to model metabolism of the species found at both nodes in the population network. Arrowheads indicate directionality. Reactions labelled v_0, v_2, v_3, v_4 have unit stoichiometry while that labelled v_1 has stoichiometry 2. Glucose, oxygen, and the fermentation product are slow metabolites whereas intracellular glucose and pyruvate are treated as fast metabolites. The reaction labelled v_3 feeds into the oxidative phosphorylation pathway, represented by OXPHOS in diagram. A full description of the EFMs associated with metabolic pathways in this metabolic network reaction network is provided by Example 1 in [34]

with $\mathbf{m}_i = (G_i, O_i, P_i)^T$ and where Q_i is the partition function used to normalise \mathbf{u}^i such that $\sum_{k=1}^3 u_k^i = 1$.

Numerical simulations of this system were performed using custom-built software based on SUNDIALS solvers [79], employing the parameter values and initial conditions displayed in Table 1. Initial conditions are chosen to model the effect of having no glucose available to the cell or sub-population at node $i = 2$ (e.g., this node might correspond to the upper layer of a colony growing on an agar substrate as in Figure 2a), but the kinetic parameter values are generic as for the related model in [34] such that no attempt has been made to fit them to experimental data. Predictions of the model should therefore be treated as purely qualitative and are intended to capture effects of the maximum entropy control law without augmentation based on additional biological knowledge, such as pathway costs that can enhance the capacity for overflow metabolism [78, 80]. Values for the diffusion coefficients reflect the fact that, while oxygen and the fermentation product are free to diffuse between nodes in the population network, glucose may not. As a consequence, the cell or sub-population at node $i = 2$ is obligatorily dependent on metabolic cross-feeding, and can only grow using the fermentation product produced from the cell or subpopulation at node $i = 1$. However, for the parameter values in Table 1, metabolic pathway $k = 3$ (glucose oxidation) has the largest zeroth-order return-on-investment when the local concentrations of glucose and oxygen are sufficiently high. Thus, biologically, the cell or sub-population at node $i = 1$ must chose between allocating greater resource towards this pathway so as to increase its own local growth rate, or assisting the cell or sub-population at node $i = 2$ to increase its local concentration of total catalytic biomass by allocating a bigger fraction of resource to metabolic pathway $k = 1$ (glucose fermentation). In the model, these choices are determined by different values of the parameter p in the cooperative metabolic objective function (4).

Results of numerical simulations are displayed in Figure 3 for various values of p , approximating the individualistic, egalitarian, elitist, and Nash regimes of cooperation, respectively. In the individualistic regime, the cell or sub-population at node $i = 2$ is still able to increase x_2 at a reasonable rate due to incidental metabolic cross-feeding that arises as a consequence of the bet-hedging nature of the individualist maximum entropy control, which models a form of diauxic growth for the cell or sub-population at node $i = 1$. When increasing the value of p towards the the elitist regime however, both the local growth rate and final local concentration of total catalytic biomass at node $i = 2$ decrease substantially. This is because the cooperative maximum entropy control disfavors metabolic cross-feeding at the dominant node in the elitist regime, and consequently there is less fermentation product available for the cell or sub-population at node $i = 2$ to grow. At the other extreme, the egalitarian regime, both the local growth rate and final local concentration of total catalytic biomass at node $i = 2$ is substantially higher than in the individualist regime. This is because the cooperative maximum entropy control favours metabolic cross-feeding at the dominant node in the egalitarian regime, and consequently there is more fermentation product available for the cell or sub-population at node $i = 2$ to grow. Remarkably, for this model, there is negligible noticeable difference between the local rates of growth at node $i = 2$ if one compares the simulation results of the egalitarian regime to those of the Nash regime, relative to the others already described. Even though the final local concentration of total catalytic biomass at node $i = 2$ achieved is slightly higher under the egalitarian cooperative maximum entropy control, the exponential phase of the x_2 trajectory is virtually indistinguishable from

that obtained in the Nash regime. This observation could indicate that the Nash regime of the cooperative metabolic objective (4) has some special biological significance perhaps attributed to its compromising egalitarian-individualist nature, but this remains to be tested by extending the model to other systems.

Table 1: Values for parameters and initial conditions used in all simulations. Values for p are reported in Figure 3.

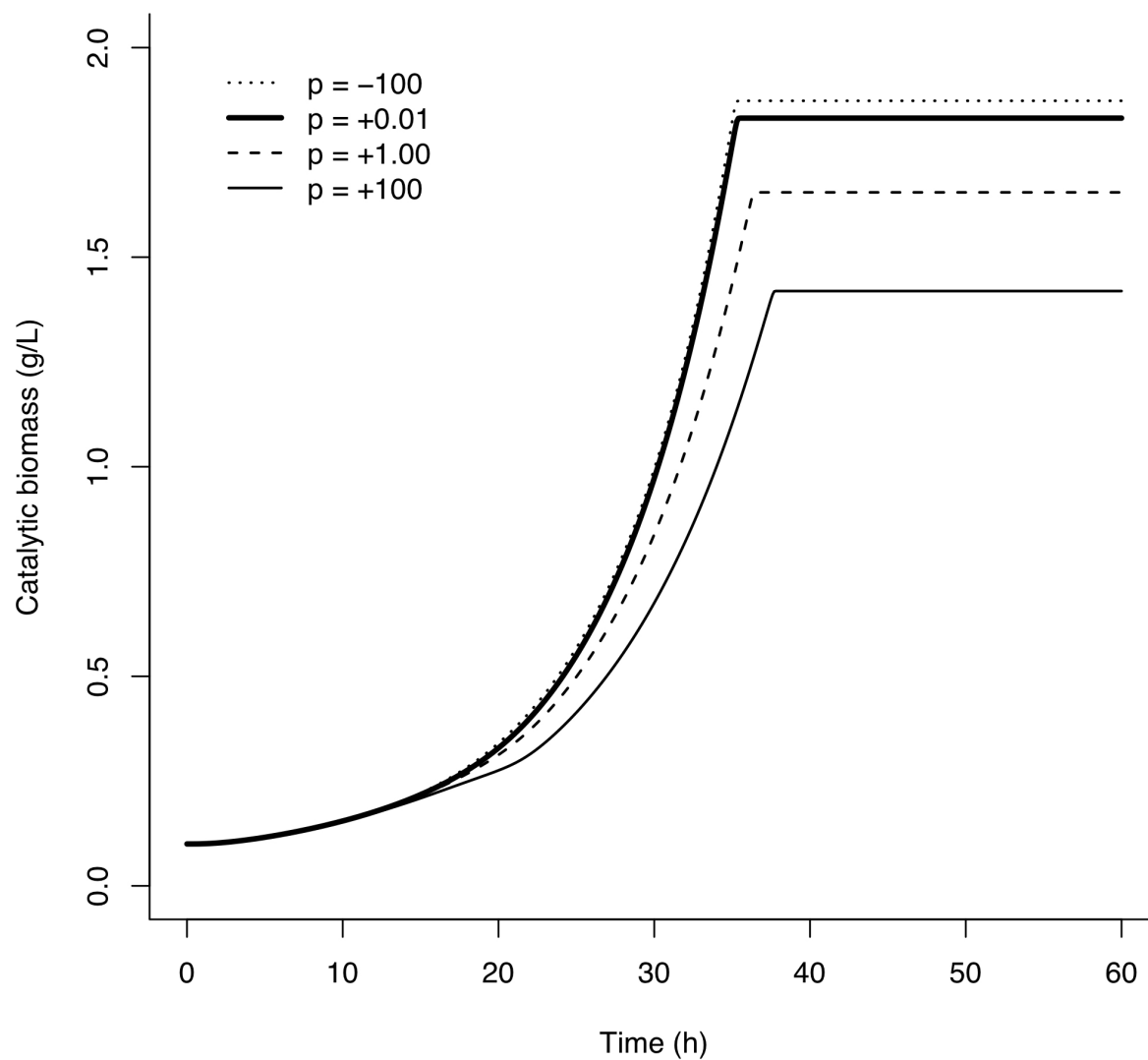
Parameters	Value	Initial conditions	Value
$V_1^{max}, V_2^{max}, V_3^{max}$	1.0 h^{-1}	$x_1(0), x_2(0)$	$0.1 \text{ g} \cdot \text{L}^{-1}$
c_1	$0.02 \text{ g} \cdot \text{g}^{-1}$	$P_1(0), P_2(0)$	$0.0 \text{ g} \cdot \text{L}^{-1}$
c_3	$0.34 \text{ g} \cdot \text{g}^{-1}$	$O_1(0), O_2(0)$	$0.0001 \text{ g} \cdot \text{L}^{-1}$
K_1, K_2, K_3	$0.01 \text{ g} \cdot \text{L}^{-1}$	$G_1(0)$	$10.0 \text{ g} \cdot \text{L}^{-1}$
$K_{O,2}, K_{O,3}$	$0.001 \text{ g} \cdot \text{L}^{-1}$	$G_2(0)$	$0.0 \text{ g} \cdot \text{L}^{-1}$
O^*	$0.015 \text{ g} \cdot \text{L}^{-1}$		
k_{La}	$30.0 \text{ g} \cdot \text{L}^{-1}$		
σ	1.0		
D_G	0.0 h^{-1}		
D_P	0.5 h^{-1}		
D_O	10.0 h^{-1}		

Although the model presented in this section provides a highly simplified description of intracellular metabolism and spatial structure in the environment or population, it has captured some fundamental yet non-trivial aspects of cooperative metabolic resource allocation in microbial systems. Extensions to accommodate metabolic models with more detailed sets of pathways can be guided using the unique recursive nature of the maximum entropy control law in combination with EFM families as described in [34]. Moreover, increased spatial complexity is also readily introduced following the procedures outlined in [19, 70, 71, 72]. In fact, in [72] a very similar dynamic model to that presented here was considered along with a rather different community-wide objective based on minimising the enthalpy of combustion in the environment. Finally, even in their current form, the dynamic and structural aspects of the model already apply to the lactate-based metabolic cross-feeding observed in higher eukaryotic organisms [11, 12, 13, 14] because of the high level of conservation in central carbon metabolism.

5 Conclusion

Organisms making regulatory decisions subject to uncertainty in future growth conditions must also contend with having very limited knowledge about their peers in spatially-structured environments and communities. In this paper, the maximum entropy control law that defines a dynamic, bet-hedging strategy for metabolic resource allocation has been extended to encompass local cooperative behaviour of individuals working together to achieve a global, population-wide metabolic objective. Analogous to the way in which the individualistic maximum entropy control predicts accumulation of metabolite reserves under growth-limiting

Figure 3: Trajectories for the local concentration of total catalytic biomass x_2 obtained from simulation of the model described in Section 4, plotted for relevant values of p corresponding to the individualistic regime ($p = 1$), the egalitarian regime ($p = -100$), the elitist regime ($p = 100$), and the Nash regime ($p = 0.01$).



conditions, its cooperative extension similarly describes when it would be optimal to allocate greater resources to pathways involved in metabolic cross-feeding over those that yield exclusive benefit to the individual. As for spatially-homogenous systems, resource fractions allocated to metabolic pathways not directly contributing to instantaneous growth (e.g., formation of storage metabolites or cross-feeding products) will tend to increase as environmental conditions become growth-limiting, but in spatially-heterogenous systems individuals may also take into consideration their current growth status relative to other community members when regulating metabolic cross-feeding. In this way, the maximum entropy principle provides a powerful framework for understanding the bet-hedging nature of dynamic metabolic resource allocation in space and time.

Acknowledgements

This work benefitted from conversations with HC Causton, L Dietrich, and MR Parsek on microbial biology and quorum sensing. DS Tourigny is a Simons Foundation Fellow of the Life Sciences Research Foundation.

A Derivation of the cooperative control law

Collecting dynamic variables into vectors $\mathbf{X}_i = (\mathbf{m}_i, x_i)^T$, the system (3) can be represented by the coupled equations $\dot{\mathbf{X}}_i = \mathbf{F}_i(\mathbf{X}, \mathbf{u}^i)$ ($i = 1, 2, \dots, \mathcal{N}$) with $\mathbf{X} = (\mathbf{X}_1, \mathbf{X}_2, \dots, \mathbf{X}_{\mathcal{N}})^T$. As in [37, 34], the individual controls \mathbf{u}^i are determined by using the linearisation of (3) about the state $\mathbf{X}(t)$ and reference controls $\{\mathbf{u}_0^i\}_{i=1,2,\dots,\mathcal{N}}$ as a good approximation for the system response at time $t + \tau$ with $\tau \in [0, \Delta t]$. The linearised equations are

$$\frac{d}{d\tau} \Delta \mathbf{X}_i = \mathbf{A}_i \Delta \mathbf{X} + \mathbf{B}_i \Delta \mathbf{u}^i + \mathbf{F}_i(\mathbf{X}(t), \mathbf{u}_0^i)$$

where

$$\mathbf{A}_i = \frac{\partial}{\partial \mathbf{X}} \mathbf{F}_i(\mathbf{X}(t), \mathbf{u}^i)$$

is the i th block row of the full Jacobian matrix \mathbf{A} and

$$\mathbf{B}_i = \frac{\partial}{\partial \mathbf{u}^i} \mathbf{F}_i(\mathbf{X}(t), \mathbf{u}^i),$$

with $\Delta \mathbf{X} = \mathbf{X}(t + \tau) - \mathbf{X}(t)$ and $\Delta \mathbf{u}^i = \mathbf{u}^i(t + \tau) - \mathbf{u}_0^i$. When the species at all nodes are identical (i.e., $\mathbf{S}_i = \mathbf{S}$, $K_i = K$, $\mathbf{c}_i = \mathbf{c}$, $r_k^i = r_k$, and $\mathbf{Z}_i^k = \mathbf{Z}^k$ for all $i = 1, 2, \dots, \mathcal{N}$) then each cooperative maximum entropy control \mathbf{u}^i is obtained by maximising the objective functional

$$\mathcal{F}_i(\mathbf{u}) = \boldsymbol{\lambda}_i^T \mathbf{B}_i \mathbf{u} + \sigma H(\mathbf{u})$$

with respect to \mathbf{u} , where

$$H(\mathbf{u}) = - \sum_{k=1}^K u_k \log(u_k)$$

is the entropy constraint and $\boldsymbol{\lambda} = (\boldsymbol{\lambda}_1, \boldsymbol{\lambda}_2, \dots, \boldsymbol{\lambda}_N)^T$ is the $\mathcal{N} \times (M + 1)$ -dimensional vector of Pontryagin co-state variables obtained by solving the boundary value problem

$$-\frac{d}{d\tau}\boldsymbol{\lambda} = \mathbf{A}^T \boldsymbol{\lambda}, \quad \boldsymbol{\lambda}(t + \Delta t) = \mathbf{q}_i.$$

The complete solution to the co-state equations is

$$\boldsymbol{\lambda}(t + \tau) = \mathbf{e}^{\mathbf{A}^T(\Delta t - \tau)} \mathbf{q}_i, \quad 0 \leq \tau \leq \Delta t,$$

but the effective return-on-investment (5) is obtained by substituting for $\boldsymbol{\lambda}$ with the heuristic $\tau = 0$ because, ultimately, only the optimal control input at the current time t is of interest [37]. Maximisation of \mathcal{F}_i proceeds as in [34] to yield the cooperative maximum entropy control (6).

An expression for the greedy effective return-on-investment is obtained by setting $\Delta t = 0$, in which case $\boldsymbol{\lambda}_i = \partial\phi_i(\mathbf{X})/\partial\mathbf{X}_i$. Moreover, $\partial\phi_i/\partial x_i$ is the only non-zero component of this vector because the cooperative objective ϕ_i does not depend on concentrations of slow metabolites. Differentiation of the generalised mean $\phi_i = M_p(\mathbf{x})$ with respect to x_i yields

$$\frac{\partial\phi_i}{\partial x_i} = \frac{x_i^{p-1}}{\sum_{j=1}^{\mathcal{N}} x_j^p} \cdot \left(\frac{1}{\mathcal{N}} \sum_{j=1}^{\mathcal{N}} x_j^p \right)^{1/p} = \frac{x_i^{p-1}}{x_i^p + y^p} \cdot M_p(\mathbf{x})$$

and the k th column of \mathbf{B}_i is

$$\mathbf{B}_i^k = x_i r_k(\mathbf{m}_i) \begin{pmatrix} \mathbf{S} \\ \mathbf{c}^T \end{pmatrix} \mathbf{Z}^k$$

so that

$$\mathcal{R}_0^{k,i} = \frac{x_i^p}{x_i^p + y^p} \cdot M_p(\mathbf{x}) \cdot r_k(\mathbf{m}_i) \mathbf{c}^T \mathbf{Z}^k.$$

This provides the greedy effective return-on-investment (7) defined using $R_0^k(\mathbf{m}_i)$ in the main text, and the resulting greedy cooperative maximum entropy control is

$$u_k^i(t) = \frac{1}{Q_i} \exp\left(\mathcal{R}_0^{k,i}/\sigma\right), \quad k = 1, 2, \dots, K$$

with $Q_i = \sum_{k=1}^K \exp(\mathcal{R}_0^{k,i}/\sigma)$. Alternative controls can be obtained in cases where the objectives ϕ_i and/or species are different across nodes in the population network, but are not considered here.

References

- [1] Axelrod R, Hamilton WD (1981) The evolution of cooperation. *Science* 211: 1390-1396.
- [2] Chao L, Levin BR (1981) Structured habitats and the evolution of anticompeteritor toxins in bacteria. *Proc. Natl. Acad. Sci. USA* 78: 6324-6328.
- [3] Nowak MA, May RM (1992) Evolutionary games and spatial chaos. *Nature* 359: 826-829.

- [4] Hansen SK, Rainey PB, Haagenzen JA, Molin S (2007) Evolution of species interactions in a biofilm community. *Nature* 445: 533-536.
- [5] Harcombe W (2010) Novel cooperation experimentally evolved between species. *Evolution* 64: 2166-2172.
- [6] Nadell CD, Foster KR, Xavier JB (2010) Emergence of spatial structure in cell groups and the evolution of cooperation. *PLoS Comput. Biol.* 6: e1000716.
- [7] Hauert C, Doebeli M (2004) Spatial structure often inhibits the evolution of cooperation in the snowdrift game. *Nature* 428: 643-646.
- [8] Oliveira NM, Niehus R, Foster KR (2014) Evolutionary limits to cooperation in microbial communities. *Proc. Natl. Acad. Sci. USA* 111: 17941-17946.
- [9] Pfeiffer T, Schuster S, Bonhoeffer S (2001) Cooperation and competition in the evolution of ATP-producing pathways. *Science* 292: 504-507.
- [10] Martin W (2010) Evolutionary origins of metabolic compartmentalization in eukaryotes. *Philos. Trans. R. Soc. Lond. B Biol. Sci.* 365: 847-855.
- [11] Nelson DL, Cox MM, Michael M (2005) Lehninger Principles of Biochemistry, 4th ed. W.H. Freeman and Company, New York. pp 543.
- [12] Bélanger M, Allaman I, Magistretti PJ (2011) Brain energy metabolism: focus on astrocyte-neuron metabolic cooperation. *Cell Metab.* 14: 724-738.
- [13] Semenza GL (2008) Tumor metabolism: cancer cells give and take lactate. *J. Clin. Invest.* 118: 3835-3837.
- [14] Lyssiotis CA, Kimmelman AC (2017) Metabolic interactions in the tumor microenvironment. *Trends Cell Biol.* 27: 863-875.
- [15] Schink B (1991) Syntrophism among prokaryotes. In: Ballows AT, HG, Dworkin M, Schleifer KH, eds. The prokaryotes. 2nd ed. Springer-Verlag, New York. pp 276-299.
- [16] Schink B (2002) Synergistic interactions in the microbial world. *Antonie Van Leeuwenhoek* 81: 257-261.
- [17] Morris BE, Henneberger R, Huber H, Moissl-Eichinger C (2013) Microbial syntrophy: interaction for the common good. *FEMS Microbiol. Rev.* 37: 384-406.
- [18] Song H-S, Cannon WR, Beliaev AS, Konopka A (2014) Mathematical modeling of microbial community dynamics: a methodological review. *Processes* 2: 711-752.
- [19] Harcombe WR, Riehl WJ, Dukovski I, Granger BR, Betts A, Lang AH, Bonilla G, Kar A, Leiby N, Mehta P, Marx CJ, Segrè D (2014) Metabolic resource allocation in individual microbes determines ecosystem interactions and spatial dynamics. *Cell Rep.* 7: 1104-1115.

- [20] Nadell CD, Drescher K, Foster KR (2016) Spatial structure, cooperation and competition in biofilms. *Nat Rev Microbiol.* 14: 589-600.
- [21] D'Souza G, Shitut S, Preussger D, Yousif G, Waschina S, Kost C (2018) Ecology and evolution of metabolic cross-feeding interactions in bacteria. *Nat. Prod. Rep.* 35: 455-488.
- [22] Lin YC, Cornell WC, Jo J, Price-Whelan A, Dietrich LEP (2018) The *Pseudomonas aeruginosa* complement of lactate dehydrogenases enables use of D- and L-lactate and metabolic cross-feeding. *mBio* 9:e00961-18.
- [23] Seger J, Brockmann HJ (1987) What is bet-hedging? In Oxford Surveys in Evolutionary Biology, Harvey PH, Partridge L (eds). Oxford University Press, Oxford. pp 182-211.
- [24] Perkins TJ, Swain PS (2009) Strategies for cellular decision-making. *Mol. Syst. Biol.* 5: 326.
- [25] Ackermann M (2015) A functional perspective on phenotypic heterogeneity in microorganisms. *Nat. Rev. Microbiol.* 13: 497-508.
- [26] Granados AA, Crane MM, Montano-Gutierrez LF, Tanaka RJ, Voliotis M, Swain PS (2017) Distributing tasks via multiple input pathways increases cellular survival in stress. *Elife* 6: e21415.
- [27] Hansen LP, Sargent TJ (2001) Robust control and model uncertainty. *Am. Econ. Rev.* 91: 60-66.
- [28] Sims, CA (2003) Implications of rational inattention. *J. Monet. Econ.* 50: 665-690.
- [29] Jaynes, ET (1957) Information theory and statistical mechanics. *Phys. Rev.* 106: 620-630.
- [30] Shore JE, Johnson RW (1980) Axiomatic derivation of the principle of maximum entropy and the principle of minimum cross-entropy. *IEEE Trans. Inf. Theory* 26: 26-37.
- [31] Shannon CE (1948) A mathematical theory of communication. *Bell Syst. Tech J.* 27: 379-423.
- [32] Harte J, Newman EA (2014) Maximum information entropy: a foundation for ecological theory. *Trends Ecol. Evol.* 29: 384-389.
- [33] Ridden SJ, Chang HH, Zygalkakis KC, MacArthur BD (2015) Entropy, ergodicity, and stem cell multipotency. *Phys. Rev. Lett.* 115: 208103.
- [34] Tourigny DS (2019) Dynamic metabolic resource allocation based on the maximum entropy principle. *arXiv preprint* arXiv:1906.03919.
- [35] De Martino D, Andersson AMC, Bergmiller B, Guet CC, Tkačik G (2017) Statistical mechanics for metabolic networks during steady state growth. *Nat. Commun.* 9: 2988.

- [36] Fernandez-de-Cossio-Diaz J, Mulet R (2019) Maximum entropy and population heterogeneity in continuous cell cultures. *PLoS Comput. Biol.* 15: e1006823.
- [37] Young JD, Ramkrishna D (2007) On the matching and proportional laws of cybernetic models. *Biotechnol. Prog.* 23: 83-99.
- [38] Young JD, Henne KL, Morgan JA, Konopka AE, Ramkrishna D (2008) Integrating cybernetic modeling with pathway analysis provides a dynamic, systems-level description of metabolic control. *Biotechnol. Bioeng.* 100: 542-559.
- [39] Mahadevan R, Edwards JS, Doyle FJ 3rd (2002) Dynamic flux balance analysis of diauxic growth in *Escherichia coli*. *Biophys. J.* 83: 1331-1340.
- [40] Provost A, Bastin, G (2004) Dynamic metabolic modelling under the balanced growth condition. *J. Process Control* 14: 717-728.
- [41] Provost A, Bastin G, Agathos SN, Schneider YJ (2006) Metabolic design of macroscopic bioreaction models: Application to Chinese hamster ovary cells. *Bioprocess Biosyst. Eng.* 29: 349-366.
- [42] Varma A, Palsson, BØ (1994) Metabolic flux balancing: basic concepts, scientific and practical use. *Nat. Biotechnol.* 12: 994-998.
- [43] Orth JD, Thiele I, Palsson, BØ (2010) What is flux balance analysis? *Nat. Biotechnol.* 28: 245-248.
- [44] Schuster S, Hilgetag C (1994) On elementary flux modes in biochemical reaction systems at steady state. *J. Biol. Syst.* 2: 165-182.
- [45] Barrat A, Barthélemy M, Vespignani A (2008) Dynamical processes on complex networks, Cambridge Univ. Press.
- [46] Othmer HG, Scriven LE (1971) Instability and dynamic pattern in cellular networks. *J. Theor. Biol.* 32: 507-537.
- [47] Othmer HG, Scriven LE (1974) Nonlinear aspects of dynamic pattern in cellular networks. *J. Theor. Biol.* 43, 83-112.
- [48] Nakao H, Mikhailov AS (2010) Turing patterns in network-organized activator-inhibitor networks. *Nature Phys.* 6: 544-550.
- [49] Bull JJ, Harcombe WR (2009) Population dynamics constrain the cooperative evolution of cross-feeding. *PLoS One* 4: e4115.
- [50] Hoek TA, Axelrod K, Biancalani T, Yurtsev EA, Liu J, Gore J (2016) Resource availability modulates the cooperative and competitive nature of a microbial cross-feeding mutualism. *PLoS Biol.* 14: e1002540.

- [51] Germerodt S, Bohl K, Lück A, Pande S, Schröter A, Kaleta C, Schuster S, Kost C (2016) Pervasive selection for cooperative cross-feeding in bacterial communities. *PLoS Comput. Biol.* 12: e1004986.
- [52] Pacheco AR, Moel M, Segré D (2019) Costless metabolic secretions as drivers of inter-species interactions in microbial ecosystems. *Nat. Commun.* 10: 103.
- [53] Pattanaik PK (2008), "Social welfare function (definition)", in Durlauf, Steven N.; Blume, Lawrence E. (eds.), *The new Palgrave dictionary of economics* (2nd ed.). Palgrave Macmillan, Basingstoke, Hampshire New York.
- [54] Nash J (1950) The bargaining problem. *Econometrica* 18: 155-162.
- [55] Miller MB, Bassler BL (2001) Quorum sensing in bacteria. *Annu. Rev. Microbiol.* 55: 165-199.
- [56] An JH, Goo E, Kim H, Seo YS, Hwang I (2014) Bacterial quorum sensing and metabolic slowing in a cooperative population. *Proc. Natl. Acad. Sci. USA* 111: 14912-14927.
- [57] Goo E, An JH, Kang Y, Hwang I (2015) Control of bacterial metabolism by quorum sensing. *Trends Microbiol.* 23: 567-576.
- [58] Davenport PW, Griffin JL, Welch M (2015) Quorum sensing is accompanied by global metabolic changes in the opportunistic human pathogen *Pseudomonas aeruginosa*. *J. Bacteriol.* 197: 2072-2082.
- [59] Boyle KE, Monaco H, van Ditmarsch D, Deforet M, Xavier JB (2015) Integration of metabolic and quorum sensing signals governing the decision to cooperate in a bacterial social trait. *PLoS Comput. Biol.* 11: e1004279.
- [60] Boyle KE, Monaco HT, Deforet M, Yan J, Wang Z, Rhee K, Xavier JB (2017) Metabolism and the evolution of social behavior. *Mol. Biol. Evol.* 34: 2367-2379.
- [61] Grote J, Krysciak D, Streit WR (2015) Phenotypic heterogeneity, a phenomenon that may explain why quorum sensing does not always result in truly homogenous cell behavior. *Appl. Environ. Microbiol.* 81: 5280-5289.
- [62] Popat R, Cornforth DM, McNally L, Brown SP (2015) Collective sensing and collective responses in quorum-sensing bacteria. *J. R. Soc. Interface* 12: 20140882.
- [63] Kussell E, Leibler S (2005) Phenotypic diversity, population growth, and information in fluctuating environments. *Science* 309: 2075-2078.
- [64] Lille SH, Pringle JR (1980) Reserve carbohydrate metabolism in *Saccharomyces cerevisiae*: responses to nutrient limitation. *J. Bacteriol.* 143: 1384-1394.
- [65] Françios J, Parrou JL (2001) Reserve carbohydrates metabolism in the yeast *Saccharomyces cerevisiae*. *FEMS Microbiol. Rev.* 25: 125-145.

- [66] Estrela S, Gudelj I (2010) Evolution of cooperative cross-feeding could be less challenging than originally thought. *PLoS One* 5: e14121.
- [67] Gardner A, West SA, Griffin AS (2007) Is bacterial persistence a social trait? *PLoS One* 2: e752.
- [68] Mulcahy LR, Isabella VM, Lewis K (2014) *Pseudomonas aeruginosa* biofilms in disease. *Microb Ecol.* 68: 1-12.
- [69] Rasamiravaka T, Labtani Q, Duez P, El Jaziri M (2015) The formation of biofilms by *Pseudomonas aeruginosa*: a review of the natural and synthetic compounds interfering with control mechanisms. *Biomed Res Int.* 2015: 759348.
- [70] Biggs MB, Papin JA (2013) Novel multiscale modeling tool applied to *Pseudomonas aeruginosa* biofilm formation. *PLoS One* 8: e78011.
- [71] Chen J, Gomez JA, Höffner K, Phalak P, Barton PI, Henson MA (2016) Spatiotemporal modeling of microbial metabolism. *BMC Syst. Biol.* 10: 21.
- [72] Zhang T, Parker A, Carlson RP, Stewart PS (2018) Flux-balance based modeling of biofilm communities. *bioRxiv preprint* doi:10.1101/441311.
- [73] Cole JA, Kohler L, Hedhli J, Luthey-Schulten Z (2015) Spatially-resolved metabolic cooperativity within dense bacterial colonies. *BMC Systems Biology* 9: 15.
- [74] Peterson JR, Cole JA, Luthey-Schulten Z (2017) Parametric studies of metabolic cooperativity in *Escherichia coli* colonies: strain and geometric confinement effects. *PLoS One* 12: e0182570.
- [75] Wolfsberg E, Long CP, Antoniewicz MR (2018) Metabolism in dense microbial colonies: ¹³C metabolic flux analysis of *E. coli* T grown on agar identifies two distinct cell populations with acetate cross-feeding. *Metab. Eng.* 49: 242-247.
- [76] Čáp M, Štěpánek L, Harant K, Váchová L, Palková Z (2012) Cell differentiation within a yeast colony: metabolic and regulatory parallels with a tumor-affected organism *Mol. Cell* 46: 436-448.
- [77] Varahan S, Walvekar A, Sinha V, Krishna S, Laxman S (2019) Metabolic constraints drive self-organization of specialized cell groups. *Elife* 8: e46735.
- [78] Möller P, Liu X, Schuster S, Boley D (2018) Linear programming model can explain respiration of fermentation products. *PLOS One* 13: e0191803.
- [79] Hindmarsh AC, Brown PN, Grant KE, Lee SL, Serban R, Shumaker DE, Woodward CS (2005) SUNDIALS: Suite of Nonlinear and Differential/Algebraic Equation Solvers. *ACM Trans. Math. Softw.* 31: 363-396.
- [80] Basan M, Hui S, Okano H, Zhang Z, Shen Y, Williamson JR, Hwa T (2015) Overflow metabolism in *Escherichia coli* results from efficient proteome allocation. *Nature* 528: 99-104.